Computation of Hydration Free Energies Using a Parameterized Continuum Model: Study of Equilibrium Geometries and Reactive Processes in Water Solution

IÑAKI TUÑÓN, MANUEL F. RUIZ-LÓPEZ,* and DANIEL RINALDI
Laboratoire de Chimie Théorique, UA CNRS 510, Université Henri Poincaré, Nancy I, BP 239, 54506 Vandoeuvre-lès-Nancy Cedex, France

JUAN BERTRÁN
Departamento de Química, Universitat Autónoma de Barcelona, 08193 Bellaterra, Spain

Received 16 March 1995; accepted 21 June 1995

ABSTRACT

A parameterized self-consistent reaction field model allowing computation of the total free energy of hydration of organic molecules at the *ab initio* level is presented. The approach uses electrostatic plus polarization energies calculated with the help of a continuum model. The remaining solvation free energy terms are obtained by a simple formula based on atomic parameters and atomic accessible surface areas (ASAs), which are determined with the ASA analytical algorithm. Analytical derivatives of the atomic surfaces areas have been implemented. The atomic parameters have been obtained by a linear regression fit of the calculated and experimental free energies of solution in water for a set of 35 molecules, leading to a standard deviation of 0.75 kcal/mol. Effects of nonelectrostatic terms on solute geometries, association energies, and activation barriers are illustrated.

*Author to whom all correspondence should be addressed.

Journal of Computational Chemistry, Vol. 17, No. 2, 148–155 (1996)

CCC 0192-8651 / 96 / 020148-08

Introduction

Several versions of the continuum solvation model have been used successfully during in recent years to compute molecular properties in solution.[1-10] These models allow a quantum treatment of the solute while the solvent is characterized by its dielectric constant (normally in the framework of the linear response theory), which leads to efficient and accurate algorithms to compute the electrostatic and polarization solvation energy. However, the calculation of other solvation energy terms, such as cavitation energy, dispersion–repulsion, hydrophobic effect, and other specific effects, is less straightforward. Nevertheless, their contribution is known to be of fundamental importance in explaining the energetics of many chemical and biochemical processes. Some attempts have been made to compute these terms, and several algorithms have been proposed to deal with the dispersion contribution at the self-consistent reaction field (SCRF) level[11,12] and to calculate dispersion–repulsion terms from atom–atom parameters through a surface integration.[13] Cavitation energy can be computed by means of the scaled particle theory[14] or by using empirically determined formulas.[15] But the main drawbacks of these methods are that they do not give a complete energetic description of the solvation process and that geometry optimizations cannot be easily done.

A simple method has been proposed to evaluate the nonelectrostatic contributions which partially avoids these problems. In this method the nonelectrostatic solvation energy, defined as the difference between the computed electrostatic plus polarization free energies and the total free energy, is obtained by means of a functional of the atomic surface areas.[8-10,16] The functional can be parameterized to reproduce some reference experimental data. This scheme is based on the proportionality between the solute's surface area and the number of solvent molecules in the first shell.[17] In this way, it has been shown that cavitation free energies are linearly well correlated to the surface area of the solute.[15] Dispersion–repulsion energies[13] are also related to the molecular surface. Finally, other energetic terms can be expected to be proportional to the number of solvent molecules placed in the first solvation shell. Thus, this approach has the advantage of recovering in an averaged way all the energy factors participating in the solvation processes. Different computational schemes have been proposed.[8-10] However, most of them are based on semiempirical Hamiltonians,[8,9] which are not always accurate enough to deal with some chemical problems. An *ab initio* scheme has also been reported, but in this case analytical geometry optimization in solution is not available.[10] In this article we present an alternative parameterization to evaluate solvation energies in water. The main advantage with respect to previous formulations is that this method allows us to carry out fast geometry optimizations of molecules in solution at the *ab initio* level, taking into account all solvation energy terms.

Methodology

Let us write the total solvation free energy as

$$\Delta G_{sol} = \Delta G_{sol}^{EP} + \Delta G_{sol}^{NE} \quad (1)$$

where ΔG_{sol}^{EP} includes the electrostatic plus polarization energies and ΔG_{sol}^{NE} all the other contributions to the solvation free energy.

In this article electrostatic plus polarization contributions have been obtained by means of a cavity model, which is briefly described later. The nonelectrostatic contribution has been obtained by the simple functional

$$\Delta G_{sol}^{NE} = \sum_i \gamma_i S_i \quad (2)$$

where S_i is the accessible surface area of atom i in the solute molecule and γ_i represents the parameters depending on atom type that are determined to fit, as well as possible, the experimental free energy of solvation of a reference set of molecules. Accessible surface areas are calculated adding the solvent radius (1.4 Å for water) to the van der Waals ones. Calculation of the area of each atom in the solute's molecules has been carried out by means of the analytical algorithm ASA.[18]

To optimize molecular geometries, the first derivatives of the nonelectrostatic term are required. They can be obtained from

$$\frac{\partial \Delta G_{sol}^{NE}}{\partial \mathbf{R}_j} = \sum_i \gamma_i \frac{\partial S_i}{\partial \mathbf{R}_j} \quad (3)$$

In this article, we have implemented an algorithm that allows us to compute surface area derivatives analytically. For this purpose, we have exploited

the fact that in the ASA algorithm[18] the accessible surface area of a given atom explicitly depends on the coordinates of the nuclei whose associated spheres are overlapping that of the atom considered. In the present version, second derivatives of the nonelectrostatic term, which are needed to compute force constants, are obtained numerically from the analytical first derivatives. The ASA algorithm[18] and the method developed to calculate surface derivatives have been implemented in a self-consistent reaction field package,[19] which is described later. *Ab initio* calculations have been carried out using the Gaussian 92 program.[20]

Parameterization Procedure

Obviously, the set of atomic parameters depends on the method used to compute the ΔG_{sol}^{EP} term. Here we propose a standard *ab initio* calculation which can be used for large molecules so that the reported parameters can be useful in a great variety of structural and reactivity studies.

The continuum model employed is that developed at Nancy.[1] The liquid is assimilated to a macroscopic continuum characterized by the dielectric constant (78.4 in the case of water). The quantum system is then placed in a cavity surrounded by this continuum. The electrostatic free energy is

$$\Delta G_{ele} = -\frac{1}{2}\sum_{l,l'=0}^{\infty}\sum_{m=-l'}^{l'}\sum_{m=-l}^{l} f_{ll'}^{mm'}\langle M_{l'}^{m'}\rangle\langle M_l^m\rangle \tag{4}$$

where M_l^m is a component of the multipole moment of order l of the gas phase structure and $f_{ll'}^{mm'}$ is a reaction field factor. In practice, good convergence is obtained by expanding the expression up to $l = 6$. This electrostatic interaction term can be included into the SCF method by introducing the corresponding perturbation to the Fock operator. Moreover, the analytical energy derivatives of the electrostatic term have been derived,[21] leading to an efficient geometry optimization procedure.[22] Hence, both the electronic and the nuclear contributions to the polarization energy can be calculated.

To compute the electrostatic plus polarization term, we have used ellipsoidal cavities whose axes are related to the axes of inertia of a solid of uniform density limited by a corrected van der Waals surface. The volume of the initial cavity is constrained to be equal to the average molecular volume in the liquid. This molecular volume is obtained by means of an empirical equation relating the van der Waals and molecular volumes.[22]

SCF calculations have been carried out at the HF/6-31G* level, which is a good compromise between accuracy and computational speed in studies of organic molecules. Geometry optimization has been carried out in the gas phase and in solution by consideration of the electrostatic term only. The influence of the nonelectrostatic solvent effect on the geometry of the molecules used for the parameterization has been found to be negligible.

Surface parameters have been obtained from linear regression analysis for a set of 35 small and medium-size neutral organic molecules containing H, C, N, and O in different functional groups. All experimental solvation free energies were taken from ref. 23. Note that these values refer to 1 molar standard state, so the computed parameters discussed later also refer to this condition. Following previous works[8] and testing different parameterization schemes, we have decided to differentiate hydrogens bonded to C, N, and O, which will be denoted as Hc, Hn, and Ho, respectively. An automatic procedure is used to determine the environment of hydrogen atoms based on interatomic distances. Nevertheless, in some particular cases (such as in the study of transition states in proton transfer processes, in which the environment of the hydrogen is not limited to a single atom), a more refined procedure must be used to avoid solvation energy discontinuities. This procedure could be based on the use of hydrogen charge–dependent parameters; this will be considered in future work.

The list of molecules used, the calculated electrostatic free energies, and the determined nonelectrostatic contributions are given in Table I. In

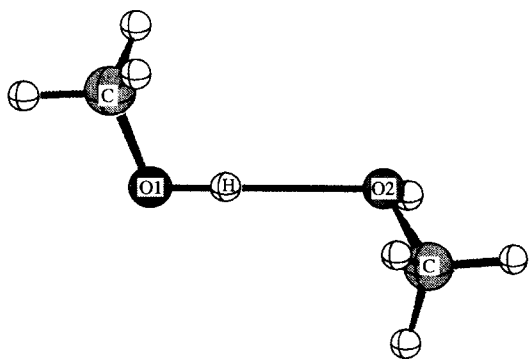

FIGURE 1. Geometry of methanol dimer.

TABLE I.
Molecules Used in the Parameterization of the Nonelectrostatic Component of the Solvation Energies.

Molecule	ΔG_{sol}^{EP}	ΔG_{sol}^{NE}	ΔG_{calc}	ΔG_{exp}	Δ
Methane	−0.16	1.00	0.84	2.00	1.16
Ethane	−0.14	1.10	0.96	1.83	0.87
Propane	−0.21	1.27	1.06	1.96	0.90
Butane	−0.15	1.42	1.27	2.08	0.81
2-Methyl butane	−0.16	1.56	1.40	2.38	0.98
Ethene	−0.98	1.49	0.51	1.27	0.76
Propene	−0.87	1.57	0.70	1.27	0.57
2-Methyl-1-propene	−0.80	1.71	0.91	1.16	0.25
Ethyne	−2.23	1.94	−0.29	−0.01	0.28
Propyne	−2.16	1.94	−0.22	−0.31	−0.09
1-Butyne	−2.08	2.00	−0.08	−0.16	−0.08
Benzene	−2.04	2.20	0.16	−0.87	−1.03
Methanol	−3.76	−1.12	−4.88	−5.11	−0.23
Ethanol	−3.14	−0.93	−4.07	−5.01	−0.94
2-Propanol	−4.09	−0.24	−4.33	−4.76	−0.43
2-Methyl-1-propanol	−3.22	−0.58	−3.80	−4.52	−0.72
1,2-ethanediol	−5.36	−2.95	−8.31	−7.66[a]	0.65
Methyl ether	−2.16	1.16	−1.00	−1.90	−0.90
Acetaldehyde	−4.48	1.04	−3.44	−3.50	−0.06
Propanal	−4.27	1.19	−3.08	−3.44	−0.36
2-Butenal	−4.91	1.62	−3.29	−4.23	−0.94
Propanone	−5.39	1.22	−4.17	−3.85	0.32
3-Pentanone	−3.67	1.53	−2.14	−3.41	−1.27
Acetic acid	−5.84	−0.88	−6.72	−6.70	0.02
Propanoic acid	−6.64	−0.75	−7.39	−6.47	0.92
Formic acid methyl ester	−4.52	1.15	−3.48	−2.78	0.70
Acetic acid methyl ester	−5.15	1.32	−3.83	−3.32	0.51
Methanamine	−3.46	−1.41	−4.87	−4.56	0.31
Ethanamine	−2.98	−1.07	−4.05	−4.50	−0.45
Propanamine	−2.78	−0.91	−3.69	−4.39	−0.70
N-methylmethanamine	−2.52	0.28	−2.24	−4.29	−2.05
1,2-Ethanediamine	−4.85	−3.60	−8.45	−7.60	0.85
Acetonitrile	−6.00	2.03	−3.97	−3.89	0.08
Propanenitrile	−6.18	2.09	−4.09	−3.85	0.24
Acetamide	−8.38	−1.26	−9.64	−9.71	−0.07

The different solvation energies—electrostatic, nonelectrostatic, calculated (sum of electrostatic and nonelectrostatic contribution), experimental, and difference Δ between the experimental and calculated energies—are given in kcal/mol. The rms standard deviation is 0.75.

[a]This is the value given in ref. 23 and used in our work. However, as a referee pointed out, a more accurate value has been reported by Suleiman et al.[28] (−9.6 kcal/mol). For a discussion of the importance of accounting for possible conformers, see the article by Cramer et al.[29]

all those molecules for which several conformers are possible, we have retained the most stable one. The root mean square (rms) standard deviation for the calculated total solvation free energies is only 0.75 kcal/mol. The optimized atomic parameters obtained from this set of molecules for Hc, Hn, Ho, C, N, and O are given in Table II. The parameters range between −60.9 and 17.2 cal/mol Å^2, in agreement with results obtained in previous works.[8] Other parameterizations[9,10] give much more negative values, but this is because cavitation energy is not included in these parameterizations but is calculated using the scaled particle theory.

The parameters proposed in Table I account for inaccuracies in the calculated electrostatic term

TABLE II.
Surface Parameters Obtained from the Set of Molecules of Table I in cal / mol Å².

Element	Bonded To	Surface Parameter
H	C	4.91
H	N	−40.68
H	O	−60.92
C	All	17.16
N	All	16.13
O	All	1.08

which are related mainly to the cavity shape and computational level used. Therefore, caution should be exercised when using these parameters with other calculation schemes. In spite of this limitation, some qualitative trends may be underlined. As expected, hydrogens atoms bonded to oxygen and nitrogen have a negative surface parameter, which can be physically interpreted from the ability to form hydrogen bonds with water molecules that are not completely included in the electrostatic term. Moreover, because of the small size of hydrogens, they do not produce an important (positive) cavitation energy term. In other words, these hydrogen atoms favor solvation, and their contribution to the free energy is a hydrophilic correction to the electrostatic plus polarization term. The surface parameter of the oxygen atom is close to zero, probably resulting from a compensation between the capability to form hydrogen bonds and dispersion energy, on one side, and cavitation and repulsion energy, on the other side. All other parameters are positive and represent a hydrophobic contribution to the free energy, the magnitude of which depends on the corresponding accessible atomic surface.

Applications

TEST OF THE ATOMIC SURFACE PARAMETERS

To test the set of parameters found, we have computed the solvation free energies of several molecules not included in the reference parameterization set and compared them to the experimental data. As before, the electrostatic energies are calculated at the HF/6-31G* level with full geometry optimization in the gas phase and in solution. Nonelectrostatic terms are obtained from eq. (2) by using the parameters given in Table II. The results for the seven molecules chosen appear in Table III. One of the molecules (nitrobenzene) has a functional group not included in the parameterization process. The root mean square standard deviation for the difference between the calculated and experimental solvation free energies of this set is 1.2 kcal/mol, which is close to the standard deviation found for the molecules parameterized. This value could be representative for the mean error expected in the calculation of solvation free energies of organic neutral molecules not considered in the parameterization. This can be considered reasonable because, in general, one is not interested in the absolute value of the solvation free energy but in a variation of this quantity in a chemical process.

INFLUENCE OF THE NONELECTROSTATIC SOLVATION ENERGY ON SOLUTE'S GEOMETRY

Some tests carried out for molecules included in the reference set have shown that nonelectrostatic effects on a solute's geometry are small. For exam-

TABLE III.
Test of the Parameterization on Some Molecules.

Molecule	ΔG_{sol}^{EP}	ΔG_{sol}^{NE}	ΔG_{calc}	ΔG_{exp}	Δ
Methoxybenzene	−2.86	2.35	−0.51	−1.04	−0.53
Cyclopentanol	−3.59	−0.26	−3.85	−5.49	−1.64
Dimethoxymethane	−4.70	1.37	−3.33	−2.93	0.40
Nitrobenzene	−4.58	1.99	−2.60	−4.12	−1.52
Acetic acid propyl ester	−5.18	1.64	−3.54	−2.86	0.68
Cyclohexene	−0.52	1.66	1.14	0.37	−0.77
Methoxyethanamine	−3.88	−0.86	−4.74	−6.55	−1.81

The different solvation energies—electrostatic, nonelectrostatic, calculated (sum of electrostatic and nonelectrostatic contribution), experimental, and difference between the experimental and calculated energies—are given in kcal / mol.

TABLE IV.
Methanol Dimer in the Gas Phase (Model I), in Water Solution Including Only Electrostatic Energy (Model II), and in Water Solution Including Electrostatic and Nonelectrostatic Interaction Energies (Model III).

Model	$d(O_1—O_2)$	$d(O_1—H)$	$d(H—O_2)$	O_1HO_2	$-\Delta E$
I	2.951	0.951	2.001	177.2	5.53
II	2.937	0.954	1.987	173.5	6.66
III	2.937	0.954	1.994	169.2	5.21

Distances in angstroms, angles in degrees, and energies in kcal / mol. O_1 and O_2 state for the proton donor and proton acceptor, respectively, (see Fig. 1).

ple, the C—O/O—H bond lengths of the methanol molecule are 1.400/0.946 Å in the gas phase, 1.406/0.948 Å in solution (considering only the electrostatic plus polarization term), and 1.405/0.949 Å (considering also the nonelectrostatic contribution). However, in weakly bonded systems, such as some dimers, the effect could be important. For this reason we have carried out optimizations of the methanol dimer in water with and without inclusion of nonelectrostatic effects.

The results of this process are given in Table IV. The inclusion of electrostatic effects produces noticeable modifications of the geometry. The oxygen–oxygen distance is shortened by 0.014 Å, and the O_1—H distance is lengthened, indicating a reinforcement of the hydrogen bond due to the polarization of the systems in solution. This stronger hydrogen bond also leads to a larger stabilization energy upon dimer formation. However, nonelectrostatic effects lengthen the O_2—H distance and deviate considerably the O_1HO_2 angle from linearity. These changes are due to the tendency of the hydrogen to expose a larger accessible surface area to the solvent in order to form hydrogen bonds with water molecules. This is not an unexpected result because the formation of the methanol proton donor–water proton acceptor dimer gives an interaction energy slightly more negative (-5.59 kcal/mol at the HF/6-31G* level) than for the methanol dimer. Therefore, because of competition with solvent water molecules, the interaction energy for the methanol dimer is somewhat smaller in solution than in the gas phase.

ACTIVATION BARRIERS

To test the influence of the nonelectrostatic contribution on chemical processes, we have selected a Diels-Alder reaction, for which hydrophobic effects are expected to play a determinant role in the activation energies.[24] The *endo-s-cis* and the *endo-s-trans* transition structures for the Diels-Alder reaction between acrolein and butadiene have been located in the gas phase and in solution with and without consideration of the nonelectrostatic solvation free energy. Exo transition states are expected to be higher in energy.[25] The geometries and the activation energies for the two transition structures are given in Table V. No appreciable change was observed for the geometry of the reagents after inclusion of nonelectrostatic forces on the electrostatically optimized structures.

From Table V it can be seen that the electrostatic term plays a crucial role on the transition structure geometries, clearly favoring the asynchronicity of the reaction in solution for both the *endo-s-cis* and the *endo-s-trans* transition structures.[25] However, nonelectrostatic effects produce modest changes in the geometry. Concerning the energy barriers, the electrostatic term favors the reaction and is the effect more pronounced for the *endo-s-cis* transition state. Nonelectrostatic effects are also important and decrease the activation energies by about 1.6 kcal/mol in both cases, without favoring one transition state with respect to the other. This hydrophobic effect on the energy barriers is in good agreement with the estimation given by Jorgensen et al.[24] in a related Diels-Alder reaction. Thus, while the electrostatic effect determines (at least in this case) the geometry and the conformation of the transition structure of the Diels-Alder reaction, nonelectrostatic effects have an important role in the activation energy and clearly contribute to the well-known acceleration of the Diels-Alder reaction in water solutions.[26] In related Diels-Alder reactions, the electrostatic solvent effect has been found to be larger for the reagents than for the transition structure.[25] However, the decrease of the barrier experimentally observed in aqueous solvent can be reproduced when the ΔG_{sol}^{NE} contribution is added to the ΔG_{sol}^{EP} term.[27]

TABLE V.
Transition Structure for the Diels-Alder Reaction between Acrolein and Butadiene in the Gas Phase (Model I), in Water Solution Including Only Electrostatic Energy (Model II), and in Water Solution Including Electrostatic and Nonelectrostatic Interaction Energies (Model III).

Model	$d1$	$d2$	$\Delta E^{\neq}$
	Endo-s-cis transition structure		
I	2.053	2.392	41.41
II	1.993	2.506	38.43
III	1.994	2.507	36.82
	Endo-s-trans transition structure		
I	2.093	2.324	42.22
II	2.019	2.431	40.37
III	2.020	2.433	38.72

$d1$ and $d2$ correspond to the two formed C—C bonds. Distances in angstroms and energy barriers in kcal / mol.

Conclusions

In this article we have presented a parameterization of nonelectrostatic solvation effects in the framework of the continuum model. The nonelectrostatic term is defined as the difference between the experimental solvation free energy and the calculated electrostatic plus polarization energy, which is obtained here at the HF/6-31G* level (including geometry optimization with electrostatic effects). The parameterization, which is based on the used of the atomic accessible surface areas and atomic surface parameters, leads to reasonable free energies of hydration, with a root mean square standard deviation between the calculated and experimental solvation free energies of only 0.75 kcal/mol.

The accessible surface areas have been calculated with the analytical ASA algorithm and analytical derivatives of the atomic areas have been implemented, allowing inclusion of nonelectrostatic analytical forces in the geometry optimization process. Nonelectrostatic solvent effects have a nearly negligible effect on geometry optimization of stable unimolecular species. For dimers, the effect on the geometry is moderate. One can also expect that in some molecular species the nonelectrostatic term could be decisive in discriminating between conformers with similar energy. In the case of the Diels-Alder reaction studied here, the influence on transition structure geometry is small. Extrapolation of this behavior to other transition structures is not obvious and deserves further work. Finally, the nonelectrostatic contribution can play an important role in the energetics of chemical processes; the magnitude of the effect is comparable in some cases to the effect of the electrostatic contribution.

Acknowledgments

The authors acknowledge Dr. D. A. Liotard for providing a copy of the ASA program and a copy of ref. 18 prior to publication. I. T. acknowledges the warm hospitality of the Laboratoire de Chimie Theorique and a postdoctoral fellowship of the Ministerio de Educación y Ciencia (MEC), Spain. M. F. R. L. and D. R. acknowledge financial support from the European Human Capital and Mobility program for a stay in the Departamento de Quimica at Barcelona.

References

1. J. L. Rivail and D. Rinaldi, *Theor. Chim. Acta*, **32**, 57 (1973).
2. O. Tapia and O. Goscinki, *Mol. Phys.*, **29**, 1653 (1975).
3. S. Miertus, E. Scrocco, and J. Tomasi, *Chem. Phys.*, **55**, 117 (1981).
4. H. Ågren, C. M. Llanos, and K. V. Mikkelsen, *Chem. Phys.*, **115**, 43 (1987).
5. H. Hoshi, M. Sakurai, Y. Inoue, and R. Chujo, *J. Chem. Phys.*, **87**, 1107 (1987).
6. G. Karlström, *J. Phys. Chem.*, **92**, 1315 (1988).
7. M. W. Wong, K. B. Wiberg, and M. J. Frisch, *J. Am. Chem. Soc.*, **114**, 523 (1992).
8. (a) C. J. Cramer and D. G. Truhlar, *J. Am. Chem. Soc.*, **113**, 8305 (1991); (b) C. J. Cramer and D. G. Truhlar, *Science*, **256**, 213 (1992); (c) C. J. Cramer and D. G. Truhlar, *J. Comput. Aided Mol. Design*, **6**, 629 (1992).
9. F. J. Luque, M. Bachs, and M. Orozco, *J. Comp. Chem.*, **15**, 847 (1994).
10. M. Bachs, F. J. Luque, and M. Orozco, *J. Comp. Chem.*, **15**, 446 (1994).
11. D. Rinaldi, B. J. Costa Cabral, and J. L. Rivail, *Chem. Phys. Letters*, **125**, 495 (1986).
12. M. A. Aguilar and F. J. Olivares del Valle, *Chem. Phys.*, **129**, 439 (1989).
13. (a) F. M. Floris and J. Tomasi, *J. Comp. Chem.*, **10**, 616 (1989); (b) F. M. Floris, J. Tomasi, and J. L. Pascual-Ahuir, *J. Comp. Chem.*, **12**, 784 (1991).
14. R. A. Pierotti, *Chem. Rev.*, **76**, 717 (1976).
15. I. Tuñón, E. Silla, and J. L. Pascual-Ahuir, *Chem. Phys. Lett.*, **203**, 289 (1993).
16. W. C. Still, A. Tempczak, R. C. Hawley, and T. Hendrickson, *J. Am. Chem. Soc.*, **112**, 6127 (1990).
17. W. L. Jorgensen, J. Gao, and C. Ravimohan, *J. Phys. Chem.*, **89**, 3470 (1985).

18. D. A. Liotard, G. D. Hawkins, G. C. Lynch, C. J. Cramer, and D. G. Truhlar, *J. Comput. Chem.*, **16**, 422 (1995).
19. D. Rinaldi and R. R. Pappalardo, SCRFPAC, QCPE, Indiana University: Bloomington, IN, 1992; program number 622.
20. M. J. Frish, G. W. Trucks, M. Head-Gordon, P. M. W. Gill, M. W. Wong, J. B. Foresman, B. G. Johnson, H. B. Schlegel, M. A. Robb, E. S. Reprogle, R. Gomperts, J. L. Andres, K. Raghavachari, J. S. Binkley, C. Gonzalez, R. L. Martin, D. J. Fox, D. J. Defrees, J. Baker, J. J. P. Stewart, and J. A. Pople, Gaussian 92, Carnegie-Mellon Quantum Chemistry Publishing Unit, Pittsburgh, PA, 1992.
21. D. Rinaldi, J. L. Rivail, and N. Rguini, *J. Comp. Chem.*, **13**, 675 (1992).
22. J. Bertrán, M. F. Ruiz-López, D. Rinaldi, and J. L. Rivail, *Theor. Chim. Acta*, **84**, 181 (1992).
23. S. Cabani, P. Gianni, V. Mollica, and L. Lepori, *J. Sol. Chem.*, **10**, 563 (1981).
24. J. F. Blake and W. L. Jorgensen, *J. Am. Chem. Soc.*, **113**, 7430 (1991).
25. M. F. Ruiz-López, X. Assfeld, J. I. Garcia, J. A. Mayoral, and L. Salvatella, *J. Am. Chem. Soc.*, **115**, 8780 (1993).
26. (a) D. C. Rideout and R. Breslow, *J. Am. Chem. Soc.*, **102**, 7816 (1980); (b) R. Breslow, U. Maitra, and D. C. Rideout, *Tetrahedron Lett.*, **24**, 1901 (1983); (c) P. A. Grieco, P. Garner, and Z. He, *Tetrahedron Lett.*, **24**, 1897 (1083); (d) P. A. Grieco, K. Yoshida, and P. Garner, *J. Org. Chem.*, **48**, 3137 (1983); (e) R. Breslow and U. Maitra, *Tetrahedron Lett.*, **25**, 1239 (1984).
27. M. F. Ruiz-López, X. Assfeld, J. I. Garcia, J. A. Mayoral, and L. Salvatella, work in progress.
28. D. Suleiman and C. A. Eckert, *J. Chem. Eng. Data*, **39**, 692 (1994).
29. C. J. Cramer and D. G. Thrular, *J. Am. Chem. Soc.*, **116**, 3892 (1994).